

X-ray diffraction and theoretical studies of the high-pressure structures and phase transitions in magnesium fluoride

J. Haines

Laboratoire de Physico-Chimie de la Matière Condensée, UMR CNRS 5617, Université Montpellier II Sciences et Techniques du Languedoc, cc 003, Place Eugène Bataillon, 34095 Montpellier cedex 5, France

J. M. Léger

Laboratoire des Propriétés Mécaniques et Thermodynamiques des Matériaux, UPR CNRS 9001, Université Paris-Nord, Avenue J. B. Clément, 93430 Villetaneuse, France

F. Gorelli

LENS and INFN, Largo Enrico Fermi 2, 50125 Florence, Italy

D. D. Klug, J. S. Tse, and Z. Q. Li

Steacie Institute for Molecular Sciences, National Research Council of Canada, Ottawa, Ontario, Canada K1A 0R6

(Received 12 March 2001; published 13 September 2001)

Magnesium fluoride is an archetypal simple ionic solid and as such has been subject to numerous theoretical studies with particular emphasis on the rutile to fluorite phase transition. In the present study by angle-dispersive, x-ray powder diffraction and density-functional plane-wave methods, it is shown that the high-pressure behavior of MgF_2 is much more complex. A second-order transition from the tetragonal rutile-type to an orthorhombic CaCl_2 -type phase is observed at 9.1 GPa, prior to the transformation at close to 14 GPa to the cubic phase, which is found to have a modified fluorite structure of the PdF_2 type. The structures of these three phases were refined by the Rietveld method, and the pressure dependence of the structural parameters is in good agreement with theory. A denser, cotunnite (α - PbCl_2)-type phase is observed at pressures above 35 GPa. Upon decompression, retransformation to the PdF_2 -type phase is observed and a mixture of the rutile- and α - PbO_2 -type forms is recovered at ambient pressure. The results of density-functional calculations yield the following sequence of stable phases: rutile \rightarrow α - PbO_2 \rightarrow PdF_2 \rightarrow α - PbCl_2 and indicate that fluorite-type structure always has a higher energy than the PdF_2 -type structure and is never stable for MgF_2 .

DOI: 10.1103/PhysRevB.64.134110

PACS number(s): 61.50.Ks, 62.50.+p, 61.10.Nz, 71.15.Mb

I. INTRODUCTION

The high-pressure behavior of magnesium fluoride is of considerable interest as this material is an archetypal simple ionic solid, which renders it particularly suitable as a test case for theoretical studies. MgF_2 , which adopts a rutile-type structure ($P4_2/mnm$, $Z=2$) under ambient conditions, is also a possible model for stishovite, the high-pressure, rutile-type form of SiO_2 . Previous theoretical calculations indicate that rutile-type MgF_2 should transform to a fluorite-type structure ($Fm\bar{3}m$, $Z=4$) at high pressure¹⁻⁶; however, up to now other possible high-pressure structures were not considered. This high-pressure, fluorite-type structure was not supported by earlier experimental results. A transition to a cubic phase was observed above 19 GPa (Ref. 7); however, the x-ray diffraction data obtained on film were not consistent with a fluorite-type structure.^{7,8} The high-pressure cubic phases of other difluorides⁸⁻¹⁰ and dioxides¹¹⁻¹⁶ have been found to have modified fluorite-type structures of the PdF_2 type, space group $Pa\bar{3}$, $Z=4$. Similarly, theoretical studies predict that silica should also adopt this structure at high pressures.¹⁷⁻²¹ Intermediate phases of the CaCl_2 ($Pnmm$, $Z=2$) and α - PbO_2 types ($Pbcn$, $Z=4$) are commonly observed in other systems between the rutile-type and modified fluorite-type forms.^{11-13,16,20,22-31} In these compounds,^{12,16} the typical sequence of high-pressure phases is

rutile \rightarrow CaCl_2 \rightarrow α - PbO_2 \rightarrow PdF_2 \rightarrow SrI_2 /orthorhombic-I- ZrO_2 \rightarrow α - PbCl_2 , with an overall increase in cation coordination number from 6 to 9.

No high-pressure structural data are available for MgF_2 , and this has motivated the present detailed structural study by angle-dispersive, x-ray powder diffraction and the investigation of the phase stability and structural parameters using density-functional theory. Magnesium fluoride presents advantages with respect other materials for both experimental and theoretical studies. The phase transitions occur at lower pressures than in many dioxides due to the higher compressibility of magnesium fluoride and the relative sizes of the constituent ions, thereby permitting these transitions to be studied under hydrostatic or close to hydrostatic conditions. In addition, the crystal structures under pressure can be determined with a high degree of precision, as the x-ray scattering from the two F^- ions is considerable with respect to that of Mg^{2+} . The highly ionic nature of MgF_2 and the absence of d electrons facilitate theoretical calculations. Magnesium fluoride is thus a good test case for experimental and theoretical methods and can serve as a model for other materials.

II. EXPERIMENT

The high-pressure, angle-dispersive, x-ray powder diffraction experiments on rutile-type MgF_2 (Alfa Products, optical

grade, purity 99.99%) were performed in a diamond anvil cell (DAC). The crystal fragments of MgF_2 were finely ground and then annealed either at 630 °C in air or at 700 °C under an argon atmosphere in order to release the stress induced in the grinding process. The resulting materials were placed in the 150- μm -diam holes which had been drilled in inconel or stainless steel gaskets preindented to a thickness of 100 μm . Powdered ruby was added as a pressure calibrant. Pressures were measured based on the shifts of the ruby R_1 and R_2 fluorescence lines.³² The 16:3:1 methanol:ethanol: H_2O (MEW) mixture was used as a hydrostatic pressure-transmitting medium in studies up to 12 GPa. At higher pressure, the samples were systematically heated using a 50-W Nd-YAG laser in order to minimize deviatoric stress. The laser beam was slowly scanned over the sample for a period of 5–15 min. The sample temperature was not measured, but was estimated to be over 1000 °C based on the visible emission observed. MgF_2 was found to react with the MEW mixture at high temperature, and thus the fluorocarbon mixture Fluorinert (3M) was used for these experiments with laser heating. The finely ground MgF_2 was very pale gray and was found to directly absorb the laser radiation at pressures up to 35 GPa. Mo_2C was added as an infrared absorber for experiments to higher pressures. In one such run, the ruby signal was found to be significantly broadened, indicating that it was in contact with the diamond anvil. The pressure was thus estimated using the equation of state of the Mo_2C with the following bulk modulus and first pressure derivative: $B_0 = 307$ GPa and $B'_0 = 6.2$ (Ref. 33).

Angle-dispersive, x-ray diffraction patterns were obtained with zirconium-filtered molybdenum radiation from an 800-W microfocus tube. X-ray capillary optics were used, giving a 100- μm -diam beam. Detection was performed with an imaging plate placed at 143.59–143.78 mm from sample.

Exposure times were typically between 48 and 60 h. A DAC in which the rear diamond was mounted over a 16°-wide slit allowing access to an angular range $4\theta = 80^\circ$ was used for these experiments. All x-ray diffraction patterns were obtained at ambient temperature. Exposures on the starting material in a 0.3-mm-diam glass capillary, and the materials recovered in the gasket after the various experiments were obtained using the same installation with sample to plate distances of 136.67–137.15 mm.

The observed intensities on the imaging plates were integrated as a function of 2θ in order to give conventional, one-dimensional diffraction profiles. Rietveld refinements were performed using the program FULLPROF.³⁴ The data for the cotunnite and α - PbO_2 -type phases could not be used for Rietveld refinements due to the low intensities of the diffraction lines and the number of variable atomic positional parameters in these structures. The individual peaks were thus fitted to pseudo-Voigt functions and unit-cell refinements were performed using the program U-FIT.³⁵ All figures in parentheses refer to the e.s.d.

III. THEORETICAL METHODS

Plane-wave total electronic energy calculations were performed with the VASP code.^{36,37} Ultrasoft Vanderbilt pseudopotentials³⁸ were used with an energy cutoff of 425 eV. All calculations were done with the generalized gradient approximation (GGA) using the Perdew-Wang exchange correlation energy.³⁹ The atomic configurations are p^6s^2 for Mg and s^2p^5 for F in the majority of calculations. Several sets of calculations were run with a s^2p^0 configuration on Mg for comparison. A $6 \times 6 \times 6$ Monkhorst-Pack⁴⁰ mesh for k -point sampling was employed for Brillouin zone integra-

TABLE I. Structural data for tetragonal, rutile-type MgF_2 [$P4_2/mnm$, $Z=2$, Mg^{2+} on $2a$ sites (0,0,0) F^- on $4f$ sites ($x,x,0$)] and orthorhombic, CaCl_2 -type MgF_2 [$Pnmm$, $Z=2$, Mg^{2+} on $2a$ sites (0,0,0) F^- on $4g$ sites ($x,y,0$)].

P (GPa)	a (Å)	b (Å)	c (Å)	x	y	$R_B/R_{\text{wp}}/R_p$ (%) ^a
Ambient	4.6249(1)		3.0520(1)	0.3027(1)		2.7/5.2/5.6
Ambient ^b	4.6213(1)		3.0519(1)	0.30293(6)		
Ambient ^c	4.628(5)		3.045(3)	0.3032(1)		
1.7	4.5967(2)		3.0376(3)	0.3018(2)		4.3/8.6/13.6
2.5	4.5871(2)		3.0300(2)	0.3011(2)		3.2/7.2/11.2
3.8	4.5716(2)		3.0220(3)	0.3005(3)		4.2/8.3/13.0
4.9	4.5503(3)		3.0132(4)	0.3006(4)		4.2/12.0/18.5
6.7	4.5294(2)		3.0007(2)	0.3002(2)		4.6/6.6/10.0
7.2	4.5224(1)		2.9985(2)	0.3004(2)		2.7/4.3/7.0
8.1	4.5128(2)		2.9932(2)	0.3001(2)		3.1/5.1/8.0
8.2	4.5105(2)		2.9912(3)	0.3005(3)		5.5/9.9/14.6
9.4	4.5164(6)	4.4768(6)	2.9845(2)	0.306(1)	0.294(1)	2.5/7.5/11.1
9.8	4.5223(16)	4.4634(15)	2.815(3)	0.309(1)	0.295(1)	5.3/9.6/14.6
10.4	4.5227(7)	4.4409(7)	2.9770(2)	0.315(1)	0.290(1)	3.9/7.7/11.3

^aAgreement factor $B = \text{Bragg}$, $p = \text{profile}$, $\text{wp} = \text{weighted profile}$.

^bSingle-crystal x-ray data (Ref. 41).

^cSingle-crystal neutron data (Ref. 42).

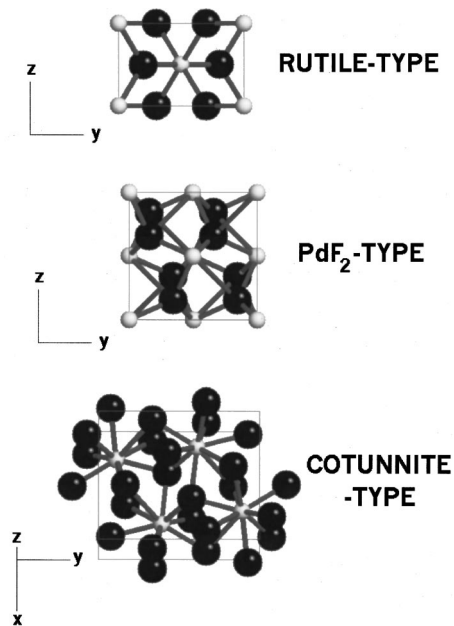


FIG. 1. Structures of rutile-type, PdF₂-type, and cotunnite-type magnesium fluoride. The CaCl₂-type structure corresponds to a very slight orthorhombic distortion of the rutile type and is not shown in the figure.

tions. All free parameters for the various structures were optimized at each volume.

IV. RESULTS AND DISCUSSION

A. Rutile-type phase

The cell constants of tetragonal, rutile-type MgF₂ (space group $P4_2/mnm$, $Z=2$) were found to be $a=4.6249(1)$ Å and $c=3.0520(1)$ Å as obtained from Rietveld refinement using the x-ray powder diffraction data obtained under ambient conditions. These values and that of the only free atomic coordinate $x(F^-)=0.3027(1)$ are in very good agreement with previous single-crystal x-ray⁴¹ and neutron⁴² diffraction studies (Table I). Under high pressure the refined value of x was found to decrease. This is similar to what has been observed in other rutile-type structures under pressure.^{13,30,43} The rutile-type structure (Fig. 1) is 20% less compressible along the c direction than in the xy plane (Fig. 2) with the mean linear compressibilities along a and c being 0.0030 and 0.0024 GPa⁻¹, respectively. The consequence of the decrease in x is that the two apical octahedral Mg-F distances in the xy plane (Fig. 3) decrease to a much greater extent than the four equatorial Mg-F distances, which bridge the cations in the chains of edge-sharing octahedra lying along the c direction. This observed decrease in x is also in agreement with the results of the theoretical calculations for the rutile-type phase (Fig. 4). It can be noted that although the use of the GGA approximation yields cell constants that are approximately 1% larger than those observed experimentally, the calculated c/a ratio at ambient pressure (0.6584) agrees well with the various experimental values (0.6580–0.6604) as do the calculated mean linear compressibilities along a (0.0030 GPa⁻¹) and c (0.0023 GPa⁻¹).

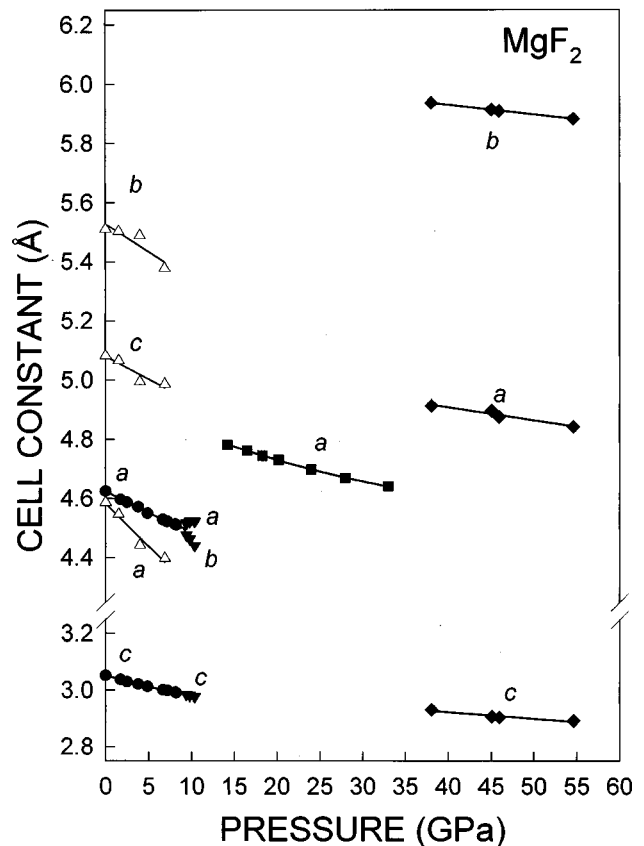


FIG. 2. Cell constants of MgF₂ as a function of pressure. Symbols correspond to rutile- (●), CaCl₂- (▼), PdF₂- (■), α -PbCl₂- (◆), and α -PbO₂- (△) type MgF₂. Solid lines represent least-squares fits to the data. The α -PbO₂-type phase was only observed on decompression.

B. CaCl₂-type phase

Rietveld refinements could no longer be successfully performed with a tetragonal rutile-type structural model at pressures above 9 GPa due to preferential broadening and subsequent splitting of the diffraction lines corresponding to the hkl ($h \neq k$) reflections of the rutile-type phase, whereas the hhl lines remained sharp (Fig. 5). This indicates that an orthorhombic distortion of the unit cell occurs in this pressure range. Similar behavior has been observed for several other rutile-type compounds,^{12–13,22–31} and the high-pressure orthorhombic phases were found to have CaCl₂-type structures ($Pnmm$, $Z=2$). Rietveld refinements using present data for orthorhombic MgF₂ indicate that the structure of this phase is also of the CaCl₂ type (Table I and Fig. 5).

Rutile-type \rightarrow CaCl₂-type phase transitions have been shown to be second order and properly ferroelastic.^{12,13,22,24,26,30,44} In the present case, no discontinuities in cell constants or volume are observed (Figs. 2 and 6), in agreement with a second-order transition. The primary order parameter for this type of tetragonal $P4_2/mnm \rightarrow Pnmm$ phase transition according to Landau theory is proportional to the spontaneous strain $e_{ss} = (a-b)/(a+b)$, where a and b are cell constants of the orthorhombic phase. It has been shown^{24,26} for this type of ferroelastic phase transition that the square of the spontaneous strain should be a linear func-

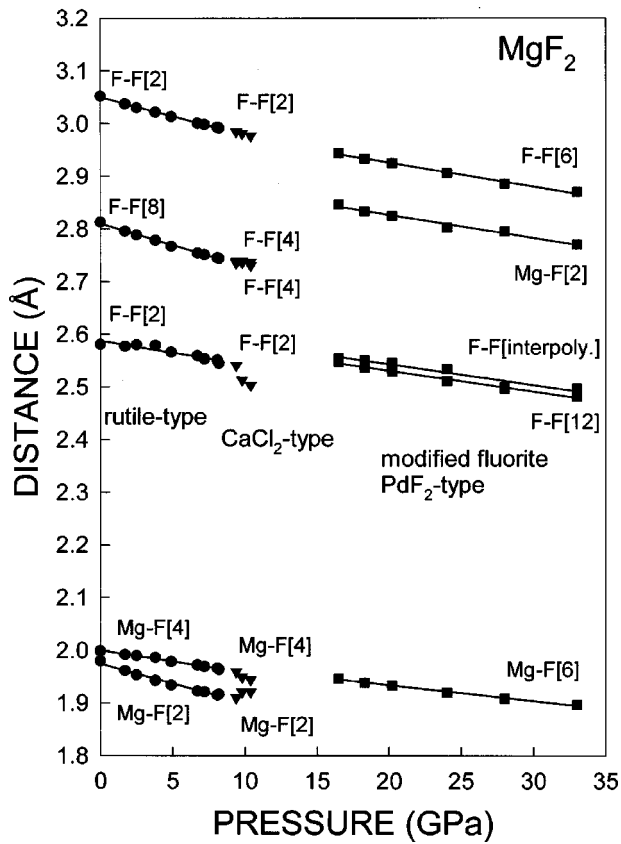


FIG. 3. Selected interatomic distances in rutile-, CaCl_2 - and PdF_2 -type MgF_2 as a function of pressure. Legend as for Fig. 2. Bond multiplicities are given in square brackets.

tion of $(P - P_c)$, where P_c is the critical pressure. This is indeed the case for CaCl_2 -type MgF_2 , and extrapolation gives a critical pressure of 9.1 GPa (Fig. 7). Slight preferential broadening was observed for the diffraction lines (hkl , $h \neq k$) that were found to split. Similar behavior^{13,26,30,45} has also been observed at ferroelastic phase transitions in other materials and is an indication of fine-scale twinning.

An additional compression mechanism is available in the orthorhombic CaCl_2 -type phase above the phase transition as the reduction in symmetry permits the columns of edge-sharing MgF_6 octahedra to tilt about their twofold axes par-

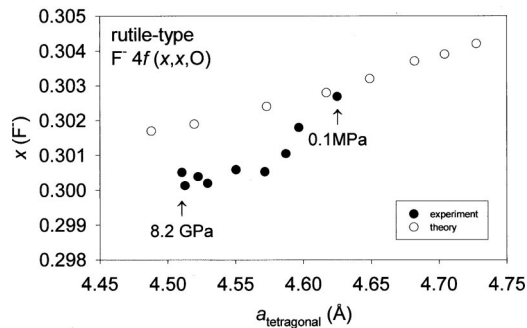


FIG. 4. Fractional x coordinate of F^- as a function of the a cell constant for rutile-type MgF_2 obtained from experiment and theory. The minimum and maximum experimental pressures are indicated.

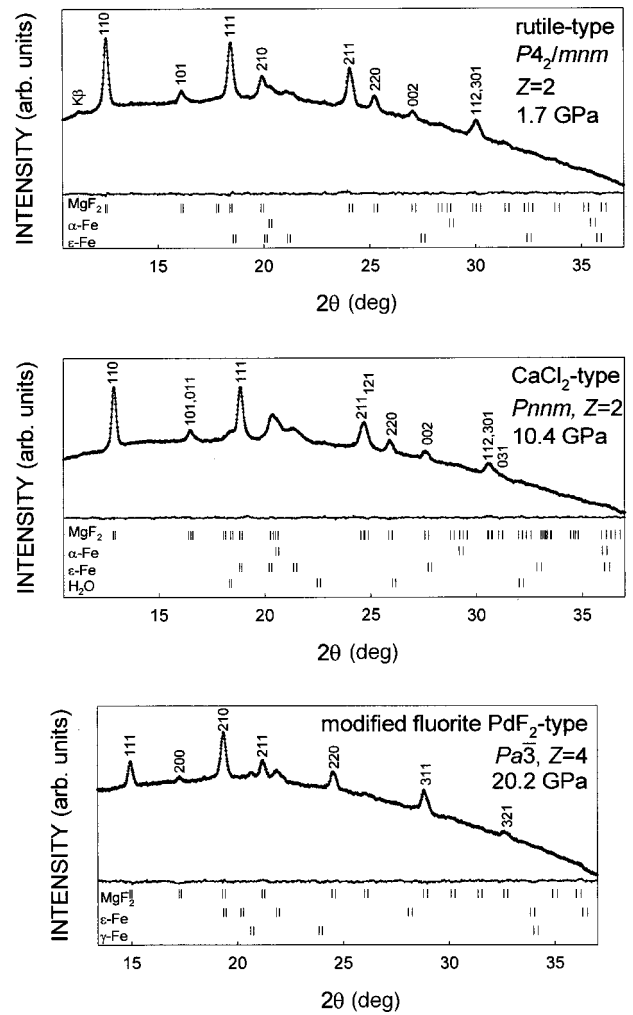


FIG. 5. Experimental data (+) and calculated profiles (solid line) from the Rietveld refinements of rutile-, CaCl_2 - and PdF_2 -type MgF_2 . The difference profiles are on the same scale. Vertical bars indicate the calculated positions of the $K\alpha_1$ and $K\alpha_2$ diffraction lines of MgF_2 , iron from the gasket (Fe), and ice from the pressure-transmitting medium (H_2O). Note that the small amount of γ -Fe at 20.2 GPa was formed at high temperature during laser heating.

allel to c . This tilting of the octahedra with respect to their orientation in the rutile-type structure can be described in terms of two angles^{46,47} ω and ω' where

$$\tan(45^\circ + \omega) = b(1/2 - y)/a(1/2 - x),$$

$$\tan(45^\circ - \omega') = by/ax.$$

These angles ω and ω' , which are zero at the phase transition, were found to increase from $\omega = 1.5(3)^\circ$ and $\omega' = 1.4(2)^\circ$ at 9.4 GPa to $\omega = 3.0(2)^\circ$ and $\omega' = 2.8(2)^\circ$ at 10.4 GPa. This corresponds to a partial collapse of the fluorine sublattice towards hexagonal close packing, which is achieved when ω reaches 10° (Ref. 48). The phase transition thus permits further densification of this material. The theoretical results also indicate that this second-order phase transition occurs, but with a slightly higher phase transition pres-

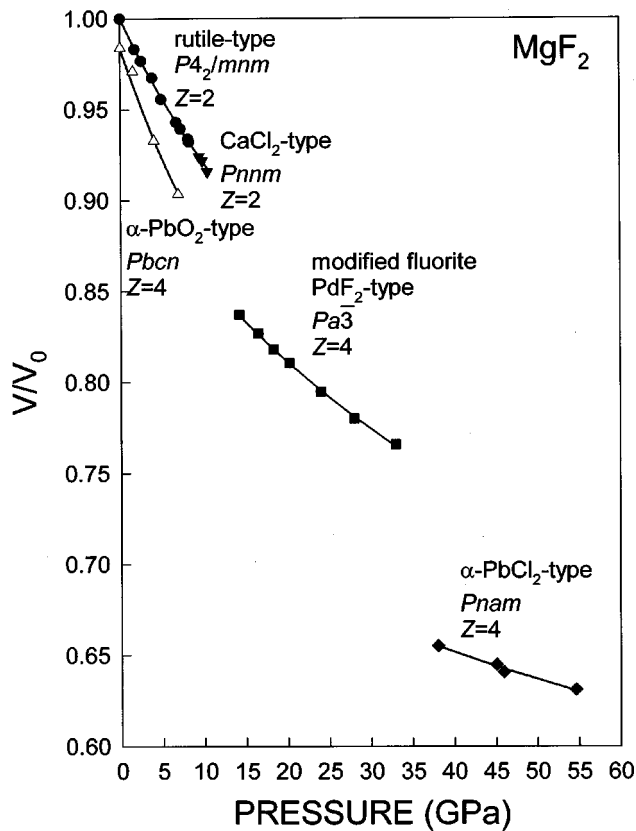


FIG. 6. Relative volume of MgF_2 as a function of pressure. Legend as for Fig. 2. Solid lines represent Birch-Murnaghan equations of state using the parameters obtained in this study.

sure of 12 GPa. The cell volume at the transition of close to 61 \AA^3 is, however, in very good agreement with experiment.

C. Modified fluorite PdF_2 -type phase

New diffraction lines were observed at pressures above 14 GPa. These lines could be readily indexed using a cubic unit cell as had previously been reported.⁷ The reflection conditions indicate that the unit cell is primitive, thereby eliminating the possibility of the fluorite-type structure ($Fm\bar{3}m$, $Z=4$) considered in previous theoretical calculations.¹⁻⁶ The most intense diffraction line observed, the 210, would in fact be absent for a fluorite-type structure. In contrast, the lines observed correspond to those allowed for a cubic, modified fluorite-type structure, space group $Pa\bar{3}$, $Z=4$, such as that obtained at high pressure for other difluorides⁸⁻¹⁰ and dioxides¹¹⁻¹⁶ such as PdF_2 , MnF_2 , RuO_2 , SnO_2 , and PbO_2 . The major difference between this structure type and fluorite concerns the fractional atomic coordinates of the anions (x,x,x), for which x is typically 0.34–0.35 for the former, whereas for the latter $x = \frac{1}{4}$. In both structures, the cations occupy a face-centered-cubic sublattice. Rietveld refinement using the data obtained at 20.2 GPa (Fig. 5 and Table II) yielded a fractional atomic coordinate $x = 0.3447(4)$ and a unit-cell parameter $a = 4.7313(2) \text{ \AA}$. The resulting coordination polyhedron is not a cube as in the case of a fluorite-type structure, but a regular rhombohedron with an edge length of

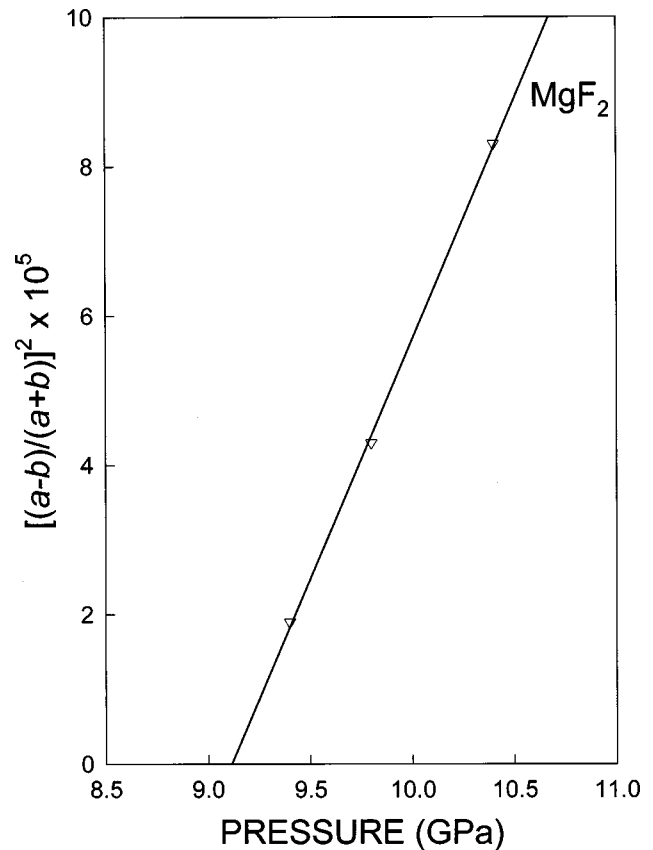


FIG. 7. Square of the spontaneous strain in CaCl_2 -type (∇) MgF_2 as a function of pressure. The line represents a least-squares fit to the data.

$2.530(2) \text{ \AA}$ and an angle $\alpha = 70.7(1)^\circ$. The magnesium cation has a coordination number of 6+2 with six fluoride anions at $1.934(2) \text{ \AA}$ and two at $2.824(2) \text{ \AA}$. The shortest interpolyhedral F-F distance of $2.546(2) \text{ \AA}$ is slightly larger than the edge of the rhombohedron. The increase in coordination number of magnesium from 6 in the CaCl_2 -type phase to 6+2 in the PdF_2 -type phase is accompanied by a decrease in volume of close to 6%.

The present density-functional theory calculations indicate that this PdF_2 -type structure is always at a lower energy than the fluorite type, which is in fact never predicted to be stable (Fig. 8). The calculated CaCl_2 -type to PdF_2 -type phase transition pressure (Table III) is 14 GPa in agreement with

TABLE II. Structural data for cubic, modified fluorite PdF_2 -type MgF_2 [$Pa\bar{3}$, $Z=4$, Mg^{2+} on $4a$ sites (0,0,0) F^- on $8c$ sites (x,x,x)].

P (GPa)	a (\AA)	x	$R_B/R_{wp}/R_p$ (%) ^a
16.5	4.7615(3)	0.3451(5)	9.9/20/28
18.3	4.7446(3)	0.3448(4)	10.5/19/26
20.2	4.7313(2)	0.3447(4)	7.0/16/25
24	4.6994(3)	0.3443(4)	9.2/19/30
28	4.6697(2)	0.3456(4)	10.0/19/30
33	4.6415(2)	0.3447(4)	9.6/19/29

^aAgreement factor $B = \text{Bragg}$, $p = \text{profile}$, $wp = \text{weighted profile}$.

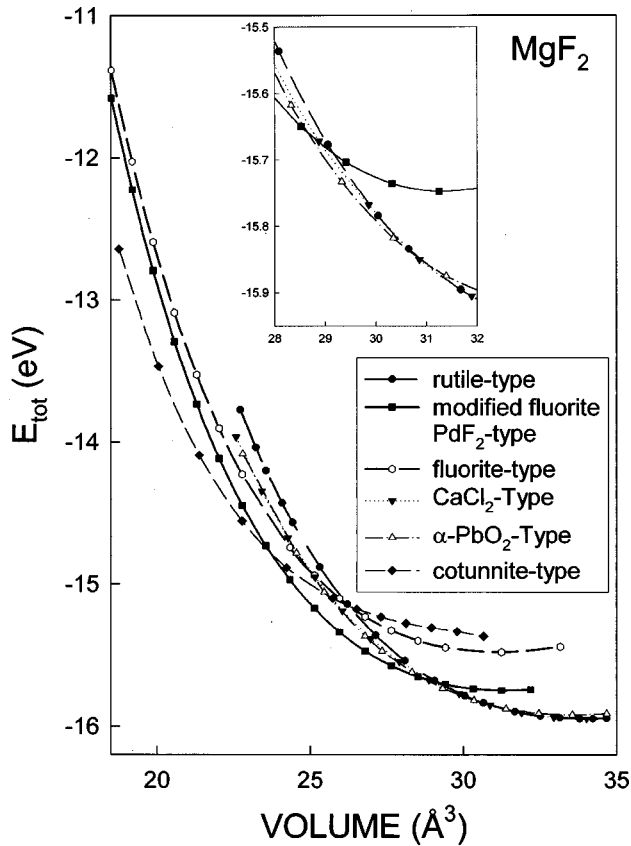


FIG. 8. Calculated total energy as a function of volume for MgF_2 in the rutile-, CaCl_2 -, PdF_2 -, $\alpha\text{-PbCl}_2$ -, $\alpha\text{-PbO}_2$ -, and fluorite-type structures.

experiment. It can be noted that the experimental value is not directly comparable to that obtained from theory as the former was obtained from measurements after laser heating. The fact that it agrees well with the equilibrium value obtained from theory indicates that the P - T slope for the phase transition is close to vertical and that the effects of thermal pressure are relatively minor. These calculations are thus in good agreement with the present experimental results and represent an important improvement with respect to the previous theoretical studies, which only considered a fluorite-type structure at high pressure.¹⁻⁶ The PdF_2 -type structure is favored over the fluorite-type structure in these compounds as it is more compact. In the fluorite structure, one-half of the cubic sites are empty, whereas in the PdF_2 -type structure

TABLE III. Experimental and theoretical phase transition pressures for MgF_2 .

Transition	$P_{\text{experiment}}$ (GPa)	P_{theory} (GPa)
rutile \rightarrow CaCl_2	9.1	12.3
rutile \rightarrow $\alpha\text{-PbO}_2$		10.9
$\text{CaCl}_2\rightarrow\alpha\text{-PbO}_2$		11.1
$\alpha\text{-PbO}_2\rightarrow\text{PdF}_2$		15
$\text{CaCl}_2\rightarrow\text{PdF}_2$	14	14
$\text{PdF}_2\rightarrow$ cotunnite	36	40

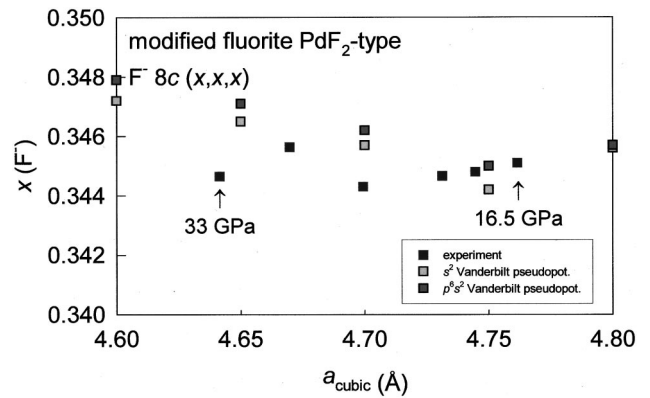


FIG. 9. Fractional x coordinate of F^- as a function of the a cell constant for PdF_2 -type MgF_2 obtained from experiment and theory. The minimum and maximum experimental pressures are indicated.

close interpolyhedral anion-anion contacts are found in the corresponding sites due to the distortion of the anion sublattice.

Recent theoretical calculations for the cubic $Pa\bar{3}$ phase of ruthenium dioxide indicate that the value of the oxygen coordinate x should increase rapidly as a function of pressure.¹⁵ The opposite trend was found in diffraction studies on RuO_2 (Refs. 14 and 15) and SnO_2 (Ref. 13). Magnesium fluoride is a much better candidate to make this type of comparison as the relative contribution of the anion to the overall diffracted intensity is much greater, thereby allowing the anion position to be determined with greater precision. In addition, the electronic configurations of the ions are particularly simple. In the cubic phase of magnesium fluoride, the results of the Rietveld refinements indicated that the x coordinate of fluorine is independent of pressure within experimental uncertainty (Fig. 9 and Table II). The theoretical calculations predict a very slight increase in x with pressure, but the values lie very close to those obtained from the structure refinements. Much better agreement is thus obtained for MgF_2 than was the case for RuO_2 . The present results cast some doubt on the magnitude of the calculated and experimental shifts in the case of RuO_2 . Questions remain as to the sign of these shifts. There is a notable difference between the structures of MgF_2 and RuO_2 in that the x coordinate of 0.35115 in the latter is significantly higher than that observed for MgF_2 and consequently the interpolyhedral anion-anion contact in RuO_2 is shorter than the intrapolyhedral contacts. The short O-O distance in cubic RuO_2 is in fact the shortest interpolyhedral O-O contact known in any oxide. The calculated increase in the x coordinate would further reduce this distance with a tendency towards a peroxide linkage. An equivalent process would not be possible in the case of MgF_2 . The experimental studies on the dioxides would indicate that their structures tend towards that of MgF_2 (i.e., $x = 0.345$) at high pressure.

D. Cotunnite ($\alpha\text{-PbCl}_2$)-type phase

A major change to the diffraction pattern of MgF_2 was observed above 35 GPa. The diffraction lines for this phase

TABLE IV. X-ray diffraction data for orthorhombic cotunnite-type ($Pnam$, $Z=4$) MgF_2 at 38 GPa. Calculated d values were obtained using the following refined cell constants: $a = 4.914(10)$ Å, $b = 5.937(9)$ Å, and $c = 2.932(6)$ Å.

d_{obs} (Å)	d_{calc} (Å)	hkl
2.533	2.541	120
1.918	1.920	121
1.893	1.893	220
1.828	1.836	130
1.799	1.795	211
1.642	1.640	031
1.579	1.579	310
1.488	1.484	040
1.465	1.466	002

could be readily indexed based on an orthorhombic unit cell (Table IV). The observed reflection conditions are in agreement with a $Pnam$ space group, and the cell constant ratios (at 38 GPa) $a/b=0.828$ and $(a+b)/c=3.70$ are characteristic of cotunnite-type structures, for which a/b ranges from 0.80 to 0.90 and $(a+b)/c$ from 3.3 to 4.0 (Refs. 49 and 50). The values for a given compound depend on the anion (oxide, halide, etc.) and the cation to anion radius ratio r_c/r_a , which ranges from 0.65 to 1.1 for this structure type in the case of halides. The radius ratio for MgF_2 is very close to this lower limit, and the observed cell constant ratios are very similar to other compounds with low r_c/r_a values such as $PbBr_2$ [$a/b=0.845$, $(a+b)/c=3.72$],⁵¹ BaI_2 [$a/b=0.834$, $(a+b)/c=3.70$],⁵² and the high-pressure form of $CaCl_2$ [$a/b=0.840$, $(a+b)/c=3.69$].⁵³ The a/b ratio for MgF_2 decreased very slightly to 0.823, whereas the $(a+b)/c$ ratio increased to 3.71 at the maximum pressure of 55 GPa. The same tendency is confirmed in the theoretical results with a/b decreasing from 0.853 to 0.834 and $(a+b)/c$ increasing from 3.65 to 3.75 over the pressure range from 44 to 227 GPa.

The transition to the cotunnite-type phase is accompanied by an increase in the magnesium coordination number from 6+2 to nine and a volume change of close to 10%. The nine fluoride ions form a tricapped trigonal prism in which cation lies. This phase was found to retransform to the PdF_2 -type phase below 35 GPa.

E. α - PbO_2 -type phase

A few additional weak-diffraction lines were observed along with those of the rutile-type phase in patterns obtained below 9 GPa on decompression from samples that had transformed to the PdF_2 -type phase at high pressure. Similar behavior was observed for SnO_2 upon decompression from the cubic phase, and the material recovered from high pressure proved to be a mixture of the rutile-type and α - PbO_2 -type phases.¹³ In the present case, the four additional lines that could be identified were found to correspond to the strongest lines of a hypothetical α - PbO_2 -type phase of MgF_2 . The following unit-cell parameters based on these four diffraction lines (110, 111, 102, and 121) were obtained at ambient pres-

sure: $a=4.587(3)$ Å, $b=5.511(3)$ Å, and $c=5.082(2)$ Å. The cell constant ratios $a/b=0.832$ and $c/b=0.922$ are very close to those calculated from theory (0.830 and 0.910) and to the corresponding values for α - PbO_2 , 0.839 and 0.919 (Ref. 54). Both experiment and theory indicate that this structure is slightly more compressible along a than in the other directions. At ambient pressure, this phase is 1.6% denser than the rutile-type form. This polymorph thus is a possible candidate for an intermediate phase between the rutile-type or $CaCl_2$ -type phases and the cubic phase. Upon heating at 7.7 GPa, however, transformation to the rutile-type phase was observed, whereas the rutile-type and $CaCl_2$ -type forms were not found to transform to the α - PbO_2 -type phase upon heating at higher pressures. The density-functional calculations clearly indicate that the α - PbO_2 -type form is the stable phase between rutile (or $CaCl_2$ -) and PdF_2 -type MgF_2 over the pressure range 11–15 GPa (Table III and Fig. 8). Based on the combined results of the present experiments and calculations, this form will have a P - T stability region lying at temperatures lower than those produced by laser heating. The mechanism concerning the formation of this phase from the cubic phase has been described in detail along with the competition with the formation of rutile-type material.¹³ The α - PbO_2 -type form can be described as a unit-cell twin of the rutile-type form, and both can thus be readily obtained on decompression from the cubic phase. In contrast, there is a high-energy barrier associated with a direct transformation between rutile (or $CaCl_2$) type MgF_2 and the α - PbO_2 -type form and this can explain why the latter is not obtained on compression at room temperature.

The present experimental and theoretical results are not inconsistent with the existence of the $CaCl_2$ -type form as the stable phase between 9.1 and 11 GPa. This form is observed experimentally, and although the calculated transition pressure is 12.1 GPa, the energy difference with respect to the rutile-type structure over this pressure range is not significant (Fig. 8). In other systems^{12,13,30} $CaCl_2$ -type phases also exhibit very limited pressure ranges of stability, and in certain cases, such as for PbO_2 (Ref. 12), this form is never stable.

F. Equations of state

The experimental P - V data for the various phases of MgF_2 were fitted to a Birch-Murnaghan equation of state (EOS) (Ref. 55):

$$P = 1.5B_0[(V/V_0)^{-7/3} - (V/V_0)^{-5/3}] \\ \times \{1 + 0.75(B'_0 - 4)[(V/V_0)^{-2/3} - 1]\},$$

where V_0 , B_0 , and B'_0 are the volume, bulk modulus, and its first derivative at ambient pressure. The calculated E - V data were well fitted using a Murnaghan EOS (Ref. 56):

$$P = (B_0/B'_0)[(V_0/V)^{B'_0} - 1].$$

The resulting values are given in Table V. It can be seen that there is very good agreement between the calculated and experimental values for the rutile-type phase, which also

TABLE V. Equation of state data for MgF₂.

Phase	Experiment			Theory		
	B_0 (GPa)	B'_0	V/V_0	B_0 (GPa)	B'_0	V/V_0
rutile	101(3)	4.2(1.1)	1.000 ^a	98	3.7	1.000 ^c
CaCl ₂				82	3.7	1.006
α -PbO ₂	69(3)	4 ^c	0.984	78	3.4	1.005
PdF ₂	123(3)	4 ^c	0.921(3)	114	3.5	0.919
cotunnite	163(35)	7 ^c	0.76(2)	158	3.5	0.813
fluorite				106	3.7	0.919

^a32.65 Å³.^b33.93 Å³.^cFixed (for most materials B'_0 typically lies between 4 and 7).

agree with previous ultrasonic values⁵⁷: $B_0 = 101.7$ GPa, $B'_0 = 3.85$. The experimental points for the CaCl₂-type phase lie on or very slightly below the extrapolated equation of state of the rutile-type phase (Fig. 6). These data taken on their own are too limited to fit to a Birch-Murnaghan equation of state. The theoretical results, on the other hand, confirm this increase in compressibility; the bulk modulus decreases by 15%. This increase in compressibility is predicted by Landau theory and can also be understood in terms of the additional compression mechanism, polyhedral tilting, which is available in the lower-symmetry orthorhombic phase. A similar increase in compressibility was also observed experimentally at the rutile-CaCl₂ transition in GeO₂ at high pressure.³⁰ Both the experimental and theoretical results concur that the α -PbO₂-type structure is the most compressible. This is similar to what was observed for metal dioxides^{12,13,58} and was attributed to the fact that this structure is built up of zigzag chains of distorted octahedra, in which the cation lies off center, rather than straight chains of cation-centered octahedra in the case of the rutile-type structure, and thus the former has more available compression mechanisms. Higher bulk moduli are observed for the denser PdF₂- and cotunnite-type phases, in which the cation coordination numbers are 6 + 2 and 9, respectively, rather than 6 in the more compressible, low-pressure forms.

G. Structural systematics in AX₂ compounds

The present understanding of rutile-type metal difluorides remains somewhat limited with respect to metal dioxides. It is well known that rutile-type compounds undergo a series of phase transitions at high pressure with increases in coordination number, leading eventually to the formation of a cotunnite-type structure.^{12,16} Previous work indicated that these compounds undergo one or more steps along one of the following phase transition pathways depending on the electronic configuration of the cation^{13,16,53,59}: rutile → CaCl₂ → α -PbO₂ → EuI₂/baddeleyite → SrI₂/orthorhombic-I-ZrO₂ → α -PbCl₂ (in the case of cations with a d^0 or d^1 electronic configuration) and rutile → CaCl₂ → α -PbO₂ → PdF₂ → SrI₂/orthorhombic-I-ZrO₂ → α -PbCl₂ (for cations with other electronic configurations).

In the case of metal difluorides, accurate high-pressure structural data are severely lacking, as are reliable theoretical

results. At present, complete, detailed information is only available for MgF₂, but it can be seen that the compound behaves in the same way as other rutile-type materials and follows in this case the second pathway, as the configuration of Mg²⁺ is $2s^22p^6$. It can be noted that in the present case, one or two steps may correspond to metastable structures. The SrI₂-type structure was not observed for MgF₂, but it may have a very narrow stability field or be present uniquely at high or low temperatures. No fluorite-type structure is observed, and the same could be expected for other rutile-type metal difluorides, which should also follow the same pathway as MgF₂.

At the present time, stishovite (rutile-type SiO₂) also appears to follow this pathway at least based on theoretical studies. Transitions to CaCl₂- and α -PbO₂-type forms have been observed experimentally in silica,^{20,23,25,29,60} but it is not yet known if only one or both are stable high-pressure forms. Stishovite was found to transform to CaCl₂-type silica above 54 GPa from *in situ* high-pressure, x-ray diffraction experiments after laser heating,²⁹ and no further transition to an α -PbO₂-type phase was observed up to 120 GPa. In contrast, in another study⁶⁰ by x-ray diffraction using cristobalite as a starting material, an α -PbO₂-like form was found to appear above 37 GPa. No CaCl₂-type phase was observed at pressures up to 90 GPa even after heating. When quartz or silica gel²⁰ were used as starting materials, mixtures of the CaCl₂- and α -PbO₂-type forms were obtained after laser heating at pressures between 68 and 85 GPa. Up to the present and as in the case of GeO₂ (Refs. 30 and 61), the high-pressure phase obtained experimentally is dependent on the starting material used. In theoretical studies,^{20,21} the CaCl₂-type form was found to have a narrow range of stability between those of the rutile- and α -PbO₂-type phases. Theoretical calculations^{18–21} indicate that at very high pressures of the order of 200 GPa, the cubic PdF₂-type form should be stable, but this has yet to be confirmed experimentally. The present work indicates that isoelectronic MgF₂ may serve as a model for the behavior of SiO₂ under these extreme conditions, both in terms of the phase transition sequence and structural evolution at high pressure.

High-pressure, postcotunnite phases with hexagonal Ni₂In- or orthorhombic-Co₂Si-related structures have been observed for a series of metal dihalides^{16,50,62–65} such as

BaX₂ (X = F, Cl, Br, I), PbX₂ (X = F, Cl), and SnCl₂. These structures are closely related to the cotunnite type; however, due to polyhedral tilting, the coordination number is 11 in the Ni₂In type and 10 in the Co₂Si type. Abrupt decreases in the orthorhombic *a/b* and (*a+b*)/*c* cell constant ratios are observed at these phase transitions, and in the lower-pressure, cotunnite-type phases these ratios already tended towards those of the final high-pressure structure. The present experiments and theoretical calculations for MgF₂ indicate that there is no tendency towards these high-density structures, and the cotunnite-type form should remain stable to at least 227 GPa. Cotunnite-type metal dioxides^{12,66} PbO₂ and ZrO₂ also do not show any tendency towards the above structure types. These high-pressure phase transitions are governed by the cation to anion radius ratio, and in these highly incompressible fluorides and dioxides, the *r_c/r_a* value will change very little up to extremely high pressures.

V. CONCLUSIONS

In contrast to previous theoretical and experimental work in which direct transformations between rutile and fluorite or rutile and distorted fluorite were considered, the present study indicates that this is not the case and that the high-pressure behavior of MgF₂ is much more complicated. The present experimental and theoretical results show that no fluorite-type phase is present for MgF₂ at high pressure. The

high-pressure, phase transition sequence for this compound is rutile→CaCl₂→α-PbO₂→PdF₂ (modified fluorite) → α-PbCl₂, with an overall increase in the coordination number of Mg²⁺ from 6 to 9. This series of phase transitions is now consistent with the structural systematics established for other AX₂ compounds. Calculations are in good agreement with respect to the transition pressures and indicate that the α-PbO₂-type phase has a pressure domain of stability between those of the rutile or CaCl₂- type and PdF₂-type forms.

Magnesium fluoride was found to be a good test case for experiment and theory as the relative scattering factors of Mg²⁺ and F⁻ enable the high-pressure positional parameters to be obtained accurately, and the ionic character of the compound and the absence of *d* electrons facilitate theoretical calculations. Both experiment and theory indicate that the fractional atomic coordinate of the fluoride ion decreases slightly with pressure in the rutile-type phase and is essentially constant in the modified fluorite-type phase. In contrast to the situation for dioxides, the compression of the modified fluorite-type phase in MgF₂ is now well understood. The present results from structure refinements at high pressure and theoretical calculations have permitted a detailed understanding of the behavior of magnesium difluoride to be obtained. This compound may serve as a model for other metal difluorides and for isoelectronic SiO₂.

- ¹J. A. Tossell, *J. Geophys. Res.* **85**, 6456 (1980).
- ²Y. A. Nga and C. K. Ong, *J. Chem. Phys.* **98**, 3240 (1993).
- ³N. L. Allan, R. I. Hines, M. D. Tower, and W. C. Mackrodt, *J. Chem. Phys.* **100**, 4710 (1994).
- ⁴K. Nishidate, M. Baba, T. Sato, and K. Nishikawa, *Phys. Rev. B* **52**, 3170 (1995).
- ⁵G. D. Barrera, M. B. Taylor, N. L. Allan, T. H. K. Barron, L. N. Kantorovich, and W. C. Mackrodt, *J. Chem. Phys.* **107**, 4337 (1997).
- ⁶E. Francisco, J. M. Recio, M. A. Blanco, A. Martín Pendás, and A. Costales, *J. Phys. Chem. A* **102**, 1595 (1998).
- ⁷L.-C. Ming and M. H. Manghnani, *Geophys. Res. Lett.* **6**, 13 (1979).
- ⁸A. Tressaud, J. L. Soubeyroux, H. Touhara, G. Demazeau, and F. Langlais, *Mater. Res. Bull.* **16**, 207 (1981).
- ⁹N. Hamaya (private communication).
- ¹⁰A. Tressaud and G. Demazeau, *High Temp.-High Press.* **16**, 303 (1984).
- ¹¹J. Haines, J. M. Léger, and O. Schulte, *Science* **271**, 629 (1996).
- ¹²J. Haines, J. M. Léger, and O. Schulte, *J. Phys.: Condens. Matter* **8**, 1631 (1996).
- ¹³J. Haines and J. M. Léger, *Phys. Rev. B* **55**, 11 144 (1997).
- ¹⁴J. Haines, J. M. Léger, M. W. Schmidt, J. P. Petit, A. S. Pereira, J. A. H. da Jornada, and S. Hull, *J. Phys. Chem. Solids* **59**, 239 (1997).
- ¹⁵J. S. Tse, D. D. Klug, K. Uehara, Z. Q. Li, J. Haines, and J. M. Léger, *Phys. Rev. B* **61**, 10 029 (2000).
- ¹⁶J. M. Léger and J. Haines, *Eur. J. Solid State Inorg. Chem.* **34**, 785 (1997).
- ¹⁷K. T. Park, K. Terakura, and Y. Matsui, *Nature (London)* **336**, 670 (1988).
- ¹⁸R. E. Cohen, in *High-Pressure Research: Applications to Earth and Planetary Sciences*, edited by Y. Syono and M. H. Manghnani (American Geophysical Union, Washington, DC, 1992), p. 425.
- ¹⁹J. S. Tse, D. D. Klug, and D. C. Allan, *Phys. Rev. B* **51**, 16 392 (1995).
- ²⁰L. S. Dubrovinsky, S. K. Saxena, P. Lazor, R. Ahuja, O. Eriksson, J. M. Wills, and B. Johansson, *Nature (London)* **388**, 362 (1997).
- ²¹D. M. Teter, R. J. Hemley, G. Kresse, and J. Hafner, *Phys. Rev. Lett.* **80**, 2145 (1998).
- ²²J. D. Jorgensen, T. G. Worlton, and J. C. Jamieson, *Phys. Rev. B* **17**, 2212 (1978).
- ²³Y. Tsuchida and T. Yagi, *Nature (London)* **340**, 217 (1989).
- ²⁴J. Haines and J. M. Léger, *Phys. Rev. B* **48**, 13 344 (1993).
- ²⁵K. J. Kingma, R. E. Cohen, R. J. Hemley, and H. K. Mao, *Nature (London)* **374**, 243 (1995).
- ²⁶J. Haines, J. M. Léger, and S. Hoyau, *J. Phys. Chem. Solids* **56**, 965 (1995).
- ²⁷J. Haines, J. M. Léger, O. Schulte, and S. Hull, *Acta Crystallogr., Sect. B: Struct. Sci.* **53**, 880 (1997).
- ²⁸J. Haines, J. M. Léger, C. Chateau, R. Bini, and L. Ulivi, *Phys. Rev. B* **58**, R2909 (1998).
- ²⁹D. Andrault, G. Fiquet, F. Guyot, and M. Hanfland, *Science* **282**, 720 (1998).
- ³⁰J. Haines, J. M. Léger, C. Chateau, and A. S. Pereira, *Phys. Chem. Miner.* **27**, 575 (2000).

- ³¹R. J. Hemley, J. Shu, M. A. Carpenter, J. Hu, H. K. Mao, and K. J. Kingma, *Solid State Commun.* **114**, 527 (2000).
- ³²H. K. Mao, J. Xu, and P. M. Bell, *J. Geophys. Res. B* **91**, 4673 (1986).
- ³³J. Haines, J. M. Léger, C. Chateau, and J. E. Lowther, *J. Phys.: Condens. Matter* **13**, 2447 (2001).
- ³⁴J. Rodríguez-Carvajal (unpublished).
- ³⁵M. Evain (unpublished).
- ³⁶G. Kress and J. Furthmuller, *Phys. Rev. B* **54**, 11 169 (1996); *Comput. Mater. Sci.* **6**, 15 (1996).
- ³⁷G. Kress and J. Hafner, *J. Phys.: Condens. Matter* **6**, 8245 (1994).
- ³⁸D. Vanderbilt, *Phys. Rev. B* **41**, 7892 (1990).
- ³⁹J. P. Perdew and A. Zunger, *Phys. Rev. B* **23**, 5048 (1981).
- ⁴⁰H. Monkhorst and J. Pack, *Phys. Rev. B* **13**, 5188 (1976).
- ⁴¹W. H. Baur, *Acta Crystallogr., Sect. B: Struct. Crystallogr. Cryst. Chem.* **32**, 2200 (1976).
- ⁴²G. Vidal-Valat, J. P. Vidal, C. M. E. Zeyen, and K. Kurki-Suonio, *Acta Crystallogr., Sect. B: Struct. Crystallogr. Cryst. Chem.* **35**, 1584 (1979).
- ⁴³N. L. Ross, J. F. Shu, R. M. Hazen, and T. Gasparik, *Am. Mineral.* **75**, 739 (1990).
- ⁴⁴M. A. Carpenter, R. J. Hemley, and H.-K. Mao, *J. Geophys. Res.* **105**, 10 807 (2000).
- ⁴⁵D. M. Adams, A. G. Christy, J. Haines, and S. M. Clark, *Phys. Rev. B* **46**, 11 358 (1992).
- ⁴⁶H. Bärninghausen, W. Bossert, and B. Anselment, *Acta Crystallogr., Sect. A: Found. Crystallogr.* **40**, C-96 (1984).
- ⁴⁷K. J. Range, F. Rau, U. Klement, and A. M. Heyns, *Mater. Res. Bull.* **22**, 1541 (1987).
- ⁴⁸W. H. Baur, *Z. Kristallogr.* **209**, 143 (1994).
- ⁴⁹H. P. Beck, *Z. Anorg. Allg. Chem.* **459**, 81 (1979).
- ⁵⁰J. M. Léger, J. Haines, A. Atouf, O. Schulte, and S. Hull, *Phys. Rev. B* **52**, 13 247 (1995).
- ⁵¹L. H. Brixner, H.-Y. Chen, and C. M. Foris, *J. Solid State Chem.* **40**, 336 (1981).
- ⁵²E. B. Brackett, T. E. Brackett, and R. L. Sass, *J. Phys. Chem.* **67**, 2132 (1963).
- ⁵³J. M. Léger, J. Haines, and C. Danneels, *J. Phys. Chem. Solids* **59**, 1199 (1998).
- ⁵⁴R. J. Hill, *Mater. Res. Bull.* **17**, 769 (1982).
- ⁵⁵F. Birch, *Phys. Rev.* **71**, 809 (1947).
- ⁵⁶F. D. Murnaghan, *Proc. Natl. Acad. Sci. U.S.A.* **30**, 244 (1944).
- ⁵⁷J. K. Vassiliou, *J. Appl. Phys.* **57**, 4543 (1985).
- ⁵⁸J. Haines and J. M. Léger, *Physica B* **192**, 233 (1993).
- ⁵⁹J. Haines, J. M. Léger, A. S. Pereira, D. Häusermann, and M. Hanfland, *Phys. Rev. B* **59**, 13 650 (1999).
- ⁶⁰L. S. Dubrovinsky, N. A. Dubrovinskaia, S. K. Saxena, F. Tutti, S. Rekh, T. Le Bihan, G. Shen, and J. Hu, *Chem. Phys. Lett.* **333**, 264 (2001).
- ⁶¹J. Haines, J. M. Léger, and C. Chateau, *Phys. Rev. B* **61**, 8701 (2000).
- ⁶²J. Haines, J. M. Léger, and O. Schulte, *Phys. Rev. B* **57**, 7551 (1998).
- ⁶³J. M. Léger, J. Haines, and A. Atouf, *Phys. Rev. B* **51**, 3902 (1995).
- ⁶⁴J. M. Léger, J. Haines, and A. Atouf, *J. Appl. Crystallogr.* **28**, 416 (1995).
- ⁶⁵J. M. Léger, J. Haines, and A. Atouf, *J. Phys. Chem. Solids* **57**, 7 (1996).
- ⁶⁶J. Haines, J. M. Léger, and A. Atouf, *J. Am. Ceram. Soc.* **78**, 445 (1995).